

STUDY OF A SILICON POWER DIODE USING A TIME DEPENDENT HYDRODYNAMIC MODEL

Received 23/01/2002 – Accepted 08/11/2003

Abstract

A one-dimensional device simulator based on the hydrodynamic model is developed for the simulation and analysis of high voltage ambipolar devices. This simulator has the capability for both self-consistent transient and steady state regime study. The discretization scheme used in the algorithm shows good numerical stability and accuracy.

A transient simulation study is carried out on a PIN diode. Information about electrical potential, electron and holes concentration, carriers temperatures, average velocities, considering the transient response to a high voltage, shows this simulator quite a good tool to study power devices in futures trends. While no significant differences appear between our results and drift diffusion model ones, for the quiescent state, it is not the case for the transient regime. Moreover, our model does not handle some strong simplification hypothesis; for instance it is pointed out that carrier explicit acceleration term can not be dodged so easily, as reported before, for an accurate transient study.

Keywords: Hydrodynamic, power diode, transient, carrier temperature, degradation.

Résumé

Un simulateur 1D est développé basé sur un modèle hydrodynamique. Il permet d'étudier des composants ambipolaires de haute tension d'une manière auto-consistante aussi bien en régime établi qu'en régime transitoire. Le schéma de discrétisation utilisé montre une bonne stabilité numérique et une bonne précision des résultats obtenus.

Une étude d'une diode PIN en régime dynamique est présentée. Les informations obtenues, relatives au potentiel électrique, à la concentration en électrons et trous, la température des porteurs et leur vitesse moyenne, en considérant la réponse transitoire, montre les capacités de ce simulateur à étudier les composants de puissance.

La comparaison de nos résultats avec ceux obtenus par le modèle DDM (Drift Diffusion Model) donne une bonne concordance en régime statique. De plus, les informations obtenues en régime dynamique n'exigent pas un recours à des hypothèses simplificatrices poussées.

Mots clés: Hydrodynamique, diode de puissance, transitoire, température des porteurs, dégradation.

S. TABIKH¹
S. LATRECHE²
H. MOREL³
C. MAILLE¹
C. GONTRAND⁴

¹ Université des Antilles
et de la Guyane

² Département d'Electronique
Faculté des Sciences de l'Ingénieur
Université Mentouri
Constantine, Algerie

³ CEGELY, INSA Lyon
20 Av. A. Einstein
69621 Villeurbanne, France

⁴ Laboratoire de Physique
de la Matière, INSA Lyon
20 Avenue A. Einstein
69621 Villeurbanne, France

ملخص

في هذا العمل قمنا بتشكيل برنامج محاكاة ذو بعد واحد بالاعتماد على نموذج هيدروديناميكي. هذا البرنامج يسمح بدراسة المركبات ثنائية الوصلات ذات توتر عالي بكيفية مترابطة، سواء في النظام الستاتيكي أو النظام الانتقالي. مخطط التقطيع المستعمل أظهر استقرارا رقميا و دقة كبيرة في النتائج المتحصل عليها.

قدمنا دراسة لثنائي المسرى PIN في النظام الديناميكي، المعلومات المتحصل عليها: التوتر الكهربائي، تركيز الإلكترونات و الثقوب، حرارة الحاملات، و سرعتها المتوسطة. بالنظر إلى الاستجابة الانتقالية تتبين قدرات هذا البرنامج في دراسة المركبات ذات الاستطاعة العالية.

مقارنة نتائجنا مع النتائج المتحصل عليها بواسطة نموذج DDM بينت لنا توافقا كبيرا في النظام الستاتيكي. بالإضافة إلى ذلك، المعلومات المتحصل عليها في النظام الديناميكي لا تستلزم الرجوع إلى فرضيات معقدة.

الكلمات المفتاحية: هيدروديناميكي، ثنائي مسرى، استطاعة، انتقالي، تدهور، حرارة الحاملات.

The PIN diode is perhaps the most widely used of all the diodes in discrete component form. It is actually a P⁺NN⁺ structure operating under high level injection conditions. It find applications varying from high voltage rectifiers to microwaves switches. Considering the current levels and the capability to evacuate the heat, this diode is much wider (a few millimetres) than high (from 80 to 100 μm). This device is often a vertical structure and can be described by one-dimensional (1D) phenomenon. Its description is involved hereafter.

The starting material is a N⁺-type bulk. An n-epitaxial layer is grown on this substrate (from 10^{13} cm^{-3} for high voltage devices, to 10^{15} cm^{-3} for low voltages). Afterwards, a boron diffusion from the surface forms a heavily doped P⁺ region. The corresponding profile is depicted on figure 1 [1]. Moreover, recombination centres of heavy metals (gold or platinum) are incorporated in this diode in order to « kill » the minority carriers. In effect, these centres reduce dramatically the life time τ_n and τ_p , about 30-100 ns in the epitaxial layer.

Most of the physical phenomena involved in this device behaviour are well described by the so-called drift-diffusion model (DDM) [2].

Unfortunately, it is rather hard to investigate the voltage strength, because of snaps occurring in the periphery of the diode and the necessity of fitting the ionisation coefficients for electron and holes, α_n and α_p respectively, which depend on the electric field E.

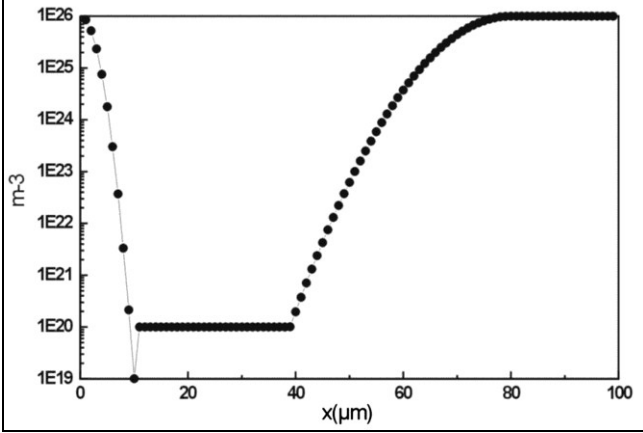


Figure 1: Doping level along the P⁺NN⁺ structure.

The field of hydrodynamic modelling has witnessed a great expansion of interest and work in recent years [3]. The hydrodynamic model (HDM) [4] appears as a good tool to improve this study, using relations less empirical, like $\alpha_n = f(T_n)$ [5]. On the other hand [6], it has been shown that T_n et T_p (electron and hole temperature) are high in the space charge layer, at the junction; It is another argument which involves the introduction of the HDM. Others fundamental reasons for introducing additional equations dealing with energy balance is the expectation that local and non-stationary effects, such as velocity overshoot, take an important place for a better understanding of devices [7]. If other algorithms, such as direct resolution of Boltzmann equations [8] or Monte Carlo simulation [9], have proved their high capability to take into account these problems, their implementation and numerical resolution are quite time consuming. An elegant manner to overcome this problem is, then, the use of an hydrodynamic model.

Moreover, a 1D modelling is sufficient and quite a good tool for our study: the power diode. It allows to investigate time dependent effects without needing an important computational effort.

Our purpose, in this paper, is mainly to present a set of equations, which are solved numerically for both self-consistent transient state and steady state simulation, applying a high voltage to the device.

1- PHYSICAL EQUATIONS

Hydrodynamic models (HDMs) [5,10] are classically based on the first three moments of the Boltzmann Transport Equation and is derived with the assumption of parabolic bands. Up to our knowledge, these models have been often applied to unipolar structures (MOSFETs, MESFETs, HEMTS,...). In this paper a transient form of HDMs is derived from carrier, momentum and energy conservation laws, for both electron and hole gases.

We start with the carrier conservation law (electron and hole continuity equations):

$$\frac{\partial n}{\partial t} + \frac{\partial(nV_n)}{\partial x} = U \quad (1)$$

$$\frac{\partial p}{\partial t} + \frac{\partial(pV_p)}{\partial x} = U \quad (2)$$

with auxiliary equations for electrons and holes:

- The momentum conservation laws:

$$n.m_n \cdot \left(\frac{\partial V_n}{\partial t} + V_n \cdot \frac{\partial V_n}{\partial x} \right) = n.e.E - \frac{\partial(n.k_B.T_n)}{\partial x} - \frac{n.m_n.V_n}{\tau_m^n} \quad (3)$$

$$p.m_p \cdot \left(\frac{\partial V_p}{\partial t} + V_p \cdot \frac{\partial V_p}{\partial x} \right) = p.e.E - \frac{\partial(p.k_B.T_p)}{\partial x} - \frac{p.m_p.V_p}{\tau_m^p} \quad (4)$$

- The energy conservation laws: (5) et (6)

$$n \left(\frac{\partial \omega_n}{\partial t} + V_n \cdot \frac{\partial \omega_n}{\partial x} \right) = n.e.E.V_n + \frac{\partial(k_B.T_n.n.V_n)}{\partial x} + \frac{\partial Q_n}{\partial x} - n \cdot \frac{\left(\omega_n - \frac{3}{2} k_B.T_L \right)}{\tau_e^n} \quad (5)$$

$$p \left(\frac{\partial \omega_p}{\partial t} + V_p \cdot \frac{\partial \omega_p}{\partial x} \right) = p.e.E.V_p - \frac{\partial(k_B.T_p.p.V_p)}{\partial x} - \frac{\partial Q_p}{\partial x} - p \cdot \frac{\left(\omega_p - \frac{3}{2} k_B.T_L \right)}{\tau_e^p} \quad (6)$$

These equations assume constant effective masses for both electrons and holes. So electron and hole momentum are $\rho_n = m_n.V_n$ and $\rho_p = m_p.V_p$, respectively. Moreover the ideal gas approximation is adopted, i.e. electron and hole gas pressure are $n.k_B.T_n$ and $p.k_B.T_p$, respectively.

A momentum conservation law may be interpreted by the mean of forces applied to the carrier gas. For instance, for an electron gas, the acceleration is $\frac{\partial V_n}{\partial t} + V_n \frac{\partial V_n}{\partial x}$, the electric force (per unity of volume) is $-enE$ and the pressure force: $-\frac{\partial(n.k_B.T_n)}{\partial x}$. The approximation of the momentum relaxation time allows to write the lattice viscous friction force as: $-\frac{n.m_n.V_n}{\tau_m^n}$. Finally, the energy

relaxation-time approximation expresses the energy losses (per unity of volume and time) due to collisions as:

$$n \frac{\left(\omega_n - \frac{3}{2} k_B.T_L \right)}{\tau_e^n}.$$

These conservation laws are completed by the classical constitutive equations for both electron and hole gases [10].

The generation term is simply the classical net recombination rate [11], which reads:

$$U = \left(\frac{\partial n}{\partial t} \right)_{coll} = \left(\frac{\partial p}{\partial t} \right)_{coll} = \frac{n.p - n_i^2}{n.\tau_p + p.\tau_n + n_i.\tau_0} \quad (7)$$

The total gas energy is the sum of the thermal and the kinetic energies,

$$\omega_n = \frac{3}{2} . k_B . T_n + \frac{1}{2} . m_n . V_n^2 \quad (8)$$

$$\omega_p = \frac{3}{2} . k_B . T_p + \frac{1}{2} . m_p . V_p^2 \quad (9)$$

On another hand, applying the heat-conduction law, yields:

$$Q_n = -\gamma_n k_B^2 n \cdot \frac{\tau_m^n}{m_n} \cdot T_n \cdot \frac{\partial T_n}{\partial x} \quad (10)$$

$$Q_p = -\gamma_p k_B^2 p \cdot \frac{\tau_m^p}{m_p} \cdot T_p \cdot \frac{\partial T_p}{\partial x} \quad (11)$$

The momentum-relaxation times are defined as [10]:

$$\tau_m^n = \frac{m_n \cdot \mu_{n0}}{e} \cdot \frac{T_L}{T_n} \quad (12)$$

$$\tau_m^p = \frac{m_p \cdot \mu_{p0}}{e} \cdot \frac{T_L}{T_p} \quad (13)$$

where $\mu_{n0} = 1400 \text{ cm}^2/\text{V.s}$ and $\mu_{p0} = 500 \text{ cm}^2/\text{V.s}$ [12,13].

The energy-relaxation times are modelled by the following equations [9],

$$\tau_e^n = \frac{m_n \cdot \mu_{n0}}{2e} \cdot \frac{T_L}{T_n} + \frac{3}{2} \cdot \frac{k_B \cdot \mu_{n0}}{e V_{nsat}^2} \cdot \frac{T_n \cdot T_L}{T_n + T_L} \quad (14)$$

$$\tau_e^p = \frac{m_p \cdot \mu_{p0}}{2e} \cdot \frac{T_L}{T_p} + \frac{3}{2} \cdot \frac{k_B \cdot \mu_{p0}}{e V_{psat}^2} \cdot \frac{T_p \cdot T_L}{T_p + T_L} \quad (15)$$

where [14],

$$V_{nsat} = 10^7 \cdot \left(\frac{T_L}{300} \right)^{-0.87} \quad \text{and} \quad V_{psat} = 8.37 \times 10^6 \cdot \left(\frac{T_L}{300} \right)^{-0.52}$$

2- NUMERICAL MODEL

Treated are, in this section, relevant numerical features. First of all, the HDM equations have to be completed by Poisson's equation,

$$\frac{\partial^2 \phi}{\partial x^2} = -\frac{e}{\epsilon_{Si}} \cdot (p - n + D_{op}) \quad (16)$$

The goal of this study is the analysis of transient behaviour of a 1D HDM for a PN junction. A simple way to account full transient phenomena is to choose the following independent variables: Φ , n , p , V_n , V_p , T_n , T_p . Notice that velocities have been chosen instead of current densities.

Using the independent variables and taking into account $E = -\frac{\partial \Phi}{\partial x}$, the independent equation set is:

$$\frac{\partial n}{\partial t} = -\frac{\partial(nV_n)}{\partial x} + U \quad (17)$$

$$\frac{\partial p}{\partial t} = -\frac{\partial(pV_p)}{\partial x} + U \quad (18)$$

$$\frac{\partial V_n}{\partial t} = -V_n \cdot \frac{\partial V_n}{\partial x} + \frac{e}{m_n} \cdot \frac{\partial \phi}{\partial x} \cdot \frac{1}{n \cdot m_n} \cdot \frac{\partial(n k_B T_n)}{\partial x} \cdot \frac{V_n}{\tau_m^n} \quad (19)$$

$$\frac{\partial V_p}{\partial t} = -V_p \cdot \frac{\partial V_p}{\partial x} + \frac{e}{m_p} \cdot \frac{\partial \phi}{\partial x} \cdot \frac{1}{p \cdot m_p} \cdot \frac{\partial(p k_B T_p)}{\partial x} \cdot \frac{V_p}{\tau_m^p} \quad (20)$$

$$\frac{\partial T_n}{\partial t} = V_n \cdot \frac{\partial T_n}{\partial x} + \frac{2}{3} \cdot \left(\frac{m_n V_n^2}{k_B \tau_m^n} - T_n \cdot \frac{\partial V_n}{\partial x} - \frac{1}{n k_B} \cdot \frac{\partial Q_n}{\partial x} - \frac{\left(\omega_n - \frac{3}{2} k_B T_L \right)}{k_B \tau_e^n} \right) \quad (21)$$

$$\frac{\partial T_p}{\partial t} = V_p \cdot \frac{\partial T_p}{\partial x} + \frac{2}{3} \cdot \left(\frac{m_p V_p^2}{k_B \tau_m^p} - T_p \cdot \frac{\partial V_p}{\partial x} - \frac{1}{p k_B} \cdot \frac{\partial Q_p}{\partial x} - \frac{\left(\omega_p - \frac{3}{2} k_B T_L \right)}{k_B \tau_e^p} \right) \quad (22)$$

The associated boundary conditions correspond to the thermodynamic equilibrium at the device boundaries:

$$p \cdot n = n_i^2 \quad (23)$$

$$T_n = T_p = T_L \quad (24)$$

The neutrality condition at the device boundaries is added, i.e: $D_{op} + p - n = 0$. Moreover the electrical potential constant is stated as:

$$\phi(t, w) = \phi_0(w) \quad (26)$$

where ϕ_0 is the thermodynamic equilibrium potential.

Lastly, the Kirchhoff Voltage Law of the circuit is applied, which gives (Fig.2):

$$e \cdot L \cdot A \cdot \frac{d}{dt} (p(t,0) V_p(t,0)) = \phi(t,0) - \phi_0(0) - V_{cc} \quad (27)$$

The initial condition is the thermodynamic equilibrium.

For numerical purpose it is useful to normalize the variables and the equations (Table 1).

variable type	variables	reference value
Potential	Φ	$u_T = \frac{k_B T_L}{e}$
Concentration	n, p	n_i
Velocity	V_n, V_p	$\sqrt{\frac{k_B T_L}{m_0}}$
Temperature	T_n, T_p	T_L
Length	x	$\sqrt{\frac{\epsilon_{Si} u_T}{e n_i}}$
Time	t	$\sqrt{\frac{\epsilon_{Si} m_0}{e^2 n_i}}$

Table 1: Normalisation of the independent variables.

Unfortunately, and contrary to the numerical classical approach of the DDM, it is not easy to use efficient numerical scheme based on Bernoulli function [5, 10],

because of the presence of $\frac{\partial V}{\partial t}$ terms. Consequently, for

both the seven equations, a classical scheme of centred finite differences is used. In practice, the mesh for the studied device contains roughly 5000 nodes, and classically the mesh step is adapted to the doping impurity profile variations (Fig.1), ie, as the doping level gradient is higher, as the step size is thinner [15]. Concerning the transient-

state simulation of this non-linear equation system, we choose the Newton-Raphson method for the sake of stability. The linearized system have been solved by a classical L.U. factorisation algorithm. No numerical oscillations are observed in the solution.

3 - SIMULATION OF A PIN JUNCTION TURN-OFF

In this section, a simulation of a PIN junction turn-off in the circuit of figure 2 is described. Figure 3 shows the transient response of the voltage drop of the PIN diode during the turn-off; The junction is biased in the inverse regime The steady state is established in roughly 150 ns.

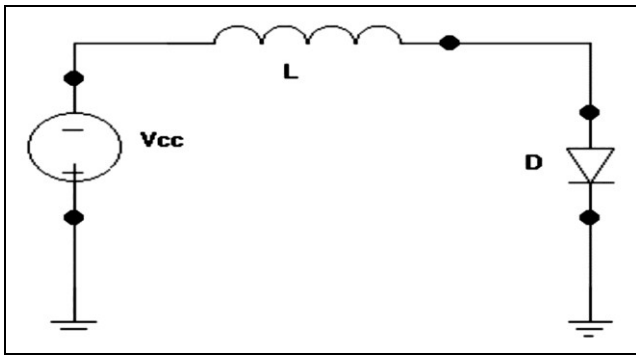


Figure 2: The PIN diode in its bias circuit.

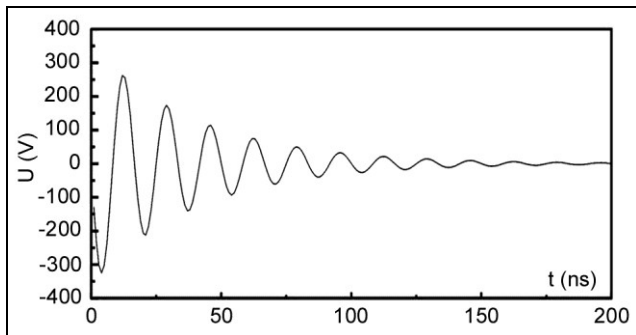


Figure 3: Voltage transient regime of the PIN diode during the turn off.

Then the output voltage between the nodes of the diode corresponds to the applied voltage (20V) and the current can be considered null (cf. saturation current). Furthermore, we can easily observe that the transient voltage can be more than twice the steady value.

First of all, the steady-state results are analysed.

On figure 4, the carrier concentrations are depicted from both DDM and HDM simulations. The different results have the same shape; The difference between the minority carrier level in the Space Charge Region (SCR) and in the N-neutral region is due to the simplified dependencies of the generation recombination model used in the HDM model. However, we can observe an amelioration for the minority carrier concentration at the boundaries of the SCR. Here intervenes the influence of carrier temperature, whom the variations are taken into account in HDM (which is not the case for DDM).

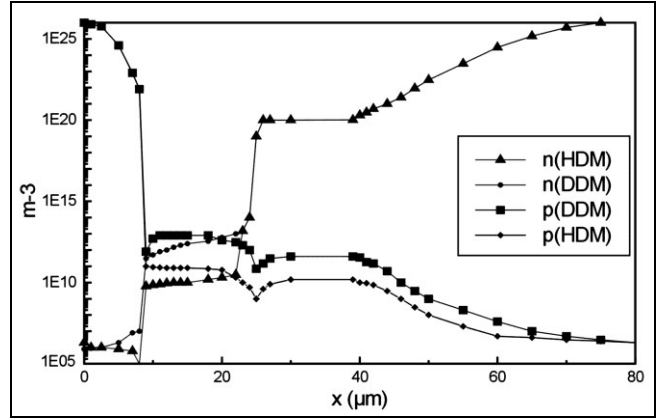


Figure 4: Carrier concentrations at the off steady state; Comparison between HDM (our model) and DDM.

On figure 5, electron and hole temperature are presented. The shape of the curves are quite similar, in the SCR, to the electric field one. As we can see, the maximum temperature reaches up to 1000 K and 520 K, for the electron and hole gases respectively. The carriers are swept away from the SCR, towards the cold (neutral) regions. But, the pressure force, induced by the high carrier concentration gradient, near but out of the junctions, opposes a strong resistance at the way out of the SCR. Although the electric field acts in the same way than the gradient temperature, it has not a significant influence on this phenomenon, since this latter does not appear when dealing with DDM.

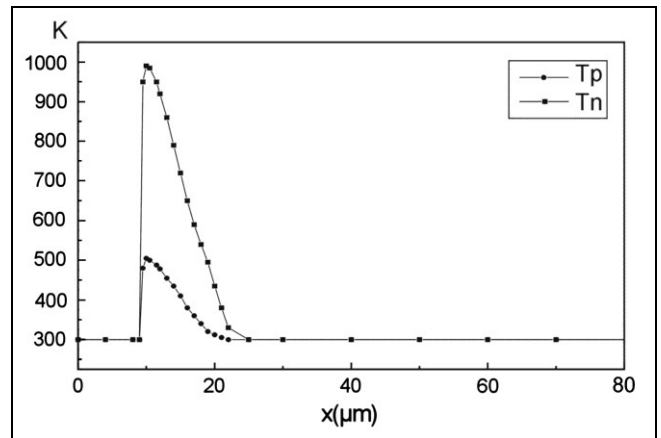


Figure 5: Electron and hole temperature versus the distance, along the structure (steady state).

On the other hand, figures 6 and 7 give the comparison between electron and hole velocity at the steady state. Classically, the carrier velocities in the SCR are high and near the saturation velocity. What more is, some peaks are observed in the velocity and temperature distributions, for minority carriers. For instance a peak in the electron velocity appears at the beginning of the SCR ($V_n = 5.10^4 \text{ m/s}$, $x = 8.6 \mu\text{m}$). For more detail, we present a zoom of this latter velocity peak. In fact, this phenomenon is clearly explained by analysing the electron momentum equation (3). We have observed that the maximum of the pressure force is very close to the boundary of the SCR,

due to a large variation of the carrier concentration, as mentioned above, and a high variation of the electron temperature in the SCR, but a low one staying in the neutral region. Moreover, since the absolute value of the electric field varies rapidly in the SCR, although we think it is of lesser importance than the one concerning the temperature, the resulting acceleration is obtained.

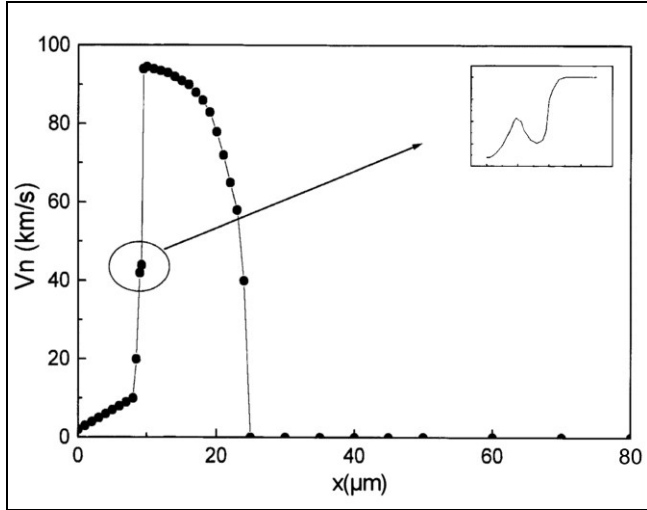


Figure 6: Electron velocity at the of steady state, versus structure depth.

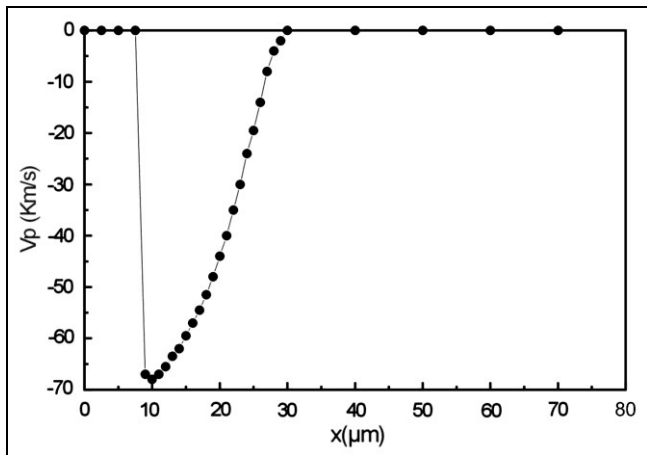


Figure 7: Hole velocity at the of steady state, versus structure depth.

Finally, small differences are observed between HDM and DDM at the steady state, and clearly they have no consequence on the external behaviour (Fig. 3). However, figure 5 point out a heating of the electron and hole gases in the SCR. That implies that it is possible to take into account ionisation phenomena using electron and hole temperature, i.e. we do believe that the ionisation generation term may be expressed using HDM variables and not using electric field as the only one criterion (cf.: the so called lucky carrier in the DDM).

Last of all, we present on figure 8 the carrier concentration at the thermodynamic equilibrium and for the steady state regime.

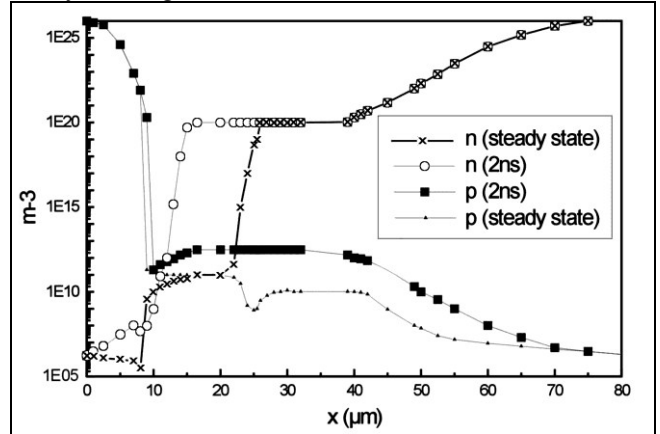


Figure 8: Carrier concentration along the PIN structure, for both thermodynamic equilibrium and steady state regime.

CONCLUSION

Simulation of a power PIN diode has been presented using a transient hydrodynamic model that includes all the main effects that govern device performance such as, for example, non-constant carrier temperature, overshoot phenomena. The greatest care must be taken in simplifying or neglecting time derivative terms, concerning the acceleration term, for instance. We have built a simulation tool which is quite efficient for analysing realistic ambipolar devices. It allows to improve the physical knowledge of such structures and to understand their electrical behaviour, in a circuit.

The future trends of our work concerns the voltage strength. We have seen the transient output voltage can be much higher than its steady value and it is a great deal with respect to the breakdown voltage point of view. More generally, non-stationary phenomena, even locally, could burden optimistic forecasts, derived only from the steady state.

In other words, it will be expected that HDM transient simulation ought to be used to predict the real device degradation.

We are now investigating high level energy phenomena, always in the framework of the hydrodynamic model. In order to develop device models with high predictive capability, it is of interest to formulate physically motivated, but computationally tractable, impact ionisation model for high-field applications.

ABBREVIATIONS

$V_{n(p)}$	Electron (hole) mean velocity;
ρ_n	Electron mean momentum;
ρ_p	Hole mean momentum;
E	Electric field;
$T_{n(p)}$	Electron (hole) temperature;
$\tau_{n(p)}$	Electron (hole) lifetime;
τ_0	Space charge region lifetime;
τ_{m}^n	Electron momentum relaxation time.;

τ_m^p	Hole momentum relaxation time;
τ_e^n	Electron energy relaxation time;
τ_e^p	Hole energy relaxation time;
$m_{n(p)}$	Electron (hole) effective mass;
$\omega_{n(p)}$	Electron (hole) mean energy;
$Q_{n(p)}$	Electron (hole) heat flow;
$\gamma_{n,p}$	Lorentz's constant(=3/2) ;
ϕ	Electric potential;
ϵ_{Si}	Silicon dielectric constant;
D_{op}	Total impurity concentration;
$\mu_{n(p)0}$	Electron (hole) low-field mobility;
$V_{n(p)sat}$	Electron (hole) saturation velocity;
T_L	Lattice temperature (=300 K);
W	Width of the simulated area;
A	Device area;
L	Inductive Load;
V_{cc}	Applied voltage;
U	Net recombination rate.

REFERENCES

- [1]- Baliga B.J., "Modern Power Devices Wiley Interscience", New York, (1987).
- [2]- Latreche S., "Etude de transistors bipolaires à émetteur polysilicium auto-aligné réalisés en technologie CMOS", Doctorat d'état, Université de Constantine, Oct. (1998).
- [3]- Grasser T., Ting-Wei Tang H., Selberherr S., "A review of hydrodynamic and energy-transport models for semiconductor device simulation", Proceedings of IEEE, Vol. 91, N°2, (2003), pp.251-274.
- [4]- Hamza M., Morel H. and Chante J.P., "A novel consistent discretization scheme for the integrated HDM/DDM simulation of semiconductor devices", Advances in mathematics and techniques, Glowinski ed., New York : Nova Science Publishers Inc., (1991), p.759-768.
- [5]- Souissi K., Odeh F., Tang H.H.K., Gnudi A., Lu P.-F., "Investigation of the Impact Ionisation in the Hydrodynamic Model", *IEEE trans. on Elec. Dev.*, Vol.40, N°8, (1997), pp.1501-1507.
- [6]- Hamza M., "Modélisation hydrodynamique des phénomènes de transport de porteurs chauds et de l'ionisation par impact dans les dispositifs à semi-conducteurs", Thèse de Doctorat, INSA de Lyon, (1993).
- [7]- Baohong Cheng Rao V.R., Woo J.C.S., "Exploration of velocity overshoot in Semiconductor", *IEEE trans. on Elec. Dev.*, Vol.20, N°10, (1999), pp.538-540.
- [8]- Schroedre D., "Modelling of interface carrier transport for device simulation", Edited by S. Selberherr, Computational Microelectronics, (1994), p. 217.
- [9]- Jungemann C., Meinerzhagen B., "On the applicability of nonself-consistent Monte Carlo device simulations", *IEEE trans. on Elec. Dev.*, Vol.49, N°6, (2002), pp.1072-1074.
- [10]- Baccarani G. and Wordmann M., "An Investigation of The Steady-State Velocity Overshoot in Silicon", *Solid State Electronics*, Vol.28, N°4, (1985), pp.407-416.
- [11]- Seeger K., "Semiconductor Physics", Ed. Springer (2002).
- [12]- Engl W. and Dorks H.K., "Models of Physical parameters", In: An Introduction to the Numerical Analysis of Semiconductor Devices and Integrated Circuits, Dublin, Boole Press, (1981), pp.223-228.
- [13]- Dorkel J.M. and Leturcq P., "Carrier Mobilities in Silicon Semi-Empirically Related to Temperature, Doping and Injection Level", *Solid State Electronics*, Vol.24, N°9, (1981), pp.821-825.
- [14]- Canali C., Majni G., Minder R. and Ottaviani G., "Electron and Hole Drift Velocity Measurements in Silicon and their Empirical Relation to Electron Field and Temperature", *IEEE Trans. Electron Devices*, Vol. ED-22, (1975), pp.1045-1047.
- [15]- MEDICI: TMA-MEDICI, two-dimensional Device Simulation Program, Technology. User's Manual, (2000). □